
BLOCK SPARSITY AND GAUGE MEDIATED WEIGHT SHARING FOR LEARNING DYNAMICAL LAWS FROM DATA

M. Götter^{1,†}, J. Fuksa², I. Roth³, and J. Eisert^{2,4}

1 Institute of Mathematics, Technische Universität Berlin, Germany

2 Dahlem Center for Complex Quantum Systems, Freie Universität Berlin, Germany

3 Quantum Research Centre, Technology Innovation Institute, Abu Dhabi

4 Fraunhofer Heinrich Hertz Institute, Germany

† goette@math.tu-berlin.de

ABSTRACT

Recent years have witnessed an increased interest in recovering dynamical laws of complex systems in a largely data-driven fashion under meaningful hypotheses. In this work, we propose a method for scalably learning dynamical laws of classical dynamical systems from data. As a novel ingredient, to achieve an efficient scaling with the system size, block sparse tensor trains – instances of tensor networks applied to function dictionaries – are used and the self similarity of the problem is exploited. For the latter, we propose an approach of gauge mediated weight sharing, inspired by notions of machine learning, which significantly improves performance over previous approaches. The practical performance of the method is demonstrated numerically on three one-dimensional systems – the Fermi-Pasta-Ulam-Tsingou system, rotating magnetic dipoles and classical particles interacting via modified Lennard-Jones potentials. We highlight the ability of the method to recover these systems, requiring 1400 samples to recover the 50 particle Fermi-Pasta-Ulam-Tsingou system to residuum of 5×10^{-7} , 900 samples to recover the 50 particle magnetic dipole chain to residuum of 1.5×10^{-4} and 7000 samples to recover the Lennard-Jones system of 10 particles to residuum 1.5×10^{-2} . The robustness against additive Gaussian noise is demonstrated for the magnetic dipole system.

Keywords Dynamical laws recovery · machine learning · tensor trains · block sparse tensor trains · tensor networks · gauge mediated weight sharing

1 Introduction

Coming-up with dynamical laws that govern the behaviour of a complex physical many-body systems has been a daunting and challenging task of great practical importance for centuries. The availability of large amounts of data and the increase in today’s computing power has drastically changed our perspective on these types of problems, shifting the focus to automated or largely ‘data-driven’ approaches [SL09, BPK16, GKES19, GGR⁺20, IMW⁺20, CPSW21, KBK22, CDA⁺21], augmented by meaningful hypotheses about the general form of the underlying dynamical laws. In this way, one can think of ‘*discovering physical laws*’ from data.

One prominent recent approach is the *sparse identification of non-linear dynamics* (SINDy) algorithm [BPK16, SBK21, dSCQ⁺20]. The state of a dynamical system is described by a set of d real variables $(x^{(1)}, \dots, x^{(d)}) =: x$, which evolve along smooth trajectories $t \mapsto x(t) \in \mathbb{R}^d$, as given by a set of d ordinary differential equations (ODE), such as

$$\dot{x}(t) = f(x(t), t) \quad \text{or} \quad \ddot{x}(t) = f(x(t), t). \quad (1)$$

The first form can be thought of as a Hamiltonian system, where $f = \{x, H\}$ with H the Hamiltonian and $\{\cdot, \cdot\}$ the Poisson bracket; the second form can be interpreted as Newton’s equations, in which case f are the forces. In this formulation, learning dynamical laws means obtaining an approximation of $f : \mathbb{R}^d \times \mathbb{R} \rightarrow \mathbb{R}^d$ from data, i.e., given M data pairs $(x_i, y_i) \in \mathbb{R}^{d \times d}$ for $i = 1, \dots, M$, with the relation $y_i \approx f(x_i)$. From now on we restrict ourselves to the case where f does not explicitly depend on time. In the SINDy approach, the learning task is phrased as a linear inversion problem. Introducing a dictionary of functions, the problem reduces to finding the coefficients that linearly combine functions in the dictionary to f . By promoting sparse solution one favours simple models and yield *interpretable* and *generalizable* results.

When applied to complex many-body systems, however, the linear parametrizations typically suffers from a drastic incarnation of the infamous *curse of dimensionality*. A naturally starting point is to generate the dictionary for each component $f_k(x) : \mathbb{R}^d \rightarrow \mathbb{R}$ of f as the product of local ansatz functions $\Psi_i : \mathbb{R} \rightarrow \mathbb{R}$, $i = 1, \dots, p$, that depend on single degrees of freedom. The multivariate dictionary is then the set of functions

$$\phi_{i_1, \dots, i_d}(x) = \Psi_{i_1}(x^{(1)}) \cdots \Psi_{i_d}(x^{(d)}), \quad (2)$$

where $x = (x^{(1)}, \dots, x^{(d)})$. As a result, we are exploring a search space of dimension exponential in d . The sparsity constraint of the SINDy approach restricts the search space to a union of lower dimensional subspaces but run-times of the original algorithm still scale with the overall dimension.

Another approach to overcome this hurdle is to identify a *physical corner* to start the search from such that one does typically not explore the entire space [GRK⁺20]. By no means do we regard all functions as equally plausible. For

example, if the range of interaction between the degrees of freedom is limited, one expects a local structure of the function dictionary that give rise to meaningful hypothesis classes. As a guiding analogy, within the context of quantum physics, *tensor networks* [CPGSV21, Oru14] have been used with overwhelming success to capture the meaningful quantum states that one is expected to find in local quantum systems [ECP10] – in instances even provably so with all rigour [SWVC08] – arriving at scalable methods. In the light of these observations a highly plausible way to do that in the present setting of learning dynamical laws is to use tensor network decompositions of the coefficient tensor Θ_k in

$$f_k(x) \approx \sum_{i_1, \dots, i_d} \Theta_{k, i_1, \dots, i_d} \phi_{i_1, \dots, i_d}(x) \quad (3)$$

and begin the search starting with low-rank decompositions. More generally speaking, locality motivates the use of *multi-linear parametrizations* [CSS15, SS16, LYCS17] introduced to the context of identifying non-linear dynamics by the *multidimensional approximation of nonlinear dynamical systems* (MANDy) method of Ref. [GKES19].

In Ref. [GRK⁺20] the idea of the starting from the physical corner has been realized by limiting the search space to different low-rank tensor-network models and using a rank-adaptive optimization algorithm. For one-dimensional systems, which are the focus of this work, tensor networks embedding *tensor trains* [BSU16] are a suitable ansatz. In this case low-rank decompositions of local systems provably exist [GRK⁺20]. Note that tensor trains have also been used to overcome the curse dimensionality in the context of many-body quantum physics, in this context referred to as *matrix product states* (MPS) [VC06, VMC08, VC04, HMOV14, CPGSV21, Oru14]; in fact, tensor trains have first been studied precisely in this context. In the many-body quantum physics introducing symmetries, such as particle number conservation, further restricts the ansatz space. In the context of tensor trains this leads to the concept of block-sparsity, see, e.g., Ref. [SPV10]. Intriguingly, bringing this concept to the multi-linear parametrizations of multivariate functions leads to natural restrictions of the function space such as bounding the polynomial degree of the approximation [BGP21, GST21].

In this work, we make use of block-sparse tensor trains for learning dynamical laws and combine them with the concept of *self-similarity* between the modes $x^{(i)}$. Self-similarity manifests itself as a redundancy of entries in the block-sparse tensor train decompositions of f_k and can be straight-forwardly enforced in our ansatz. We show that carefully exploiting the *gauge freedom* of the tensor train decomposition yields a highly scalable and numerically stable algorithmic approach for recovering dynamical laws. To this end, we introduce a new method coined *gauge mediated weight sharing*. The term is borrowed from a related concept in *machine learning* [RCR⁺20]. The key observation leading to *gauge mediated weight sharing* is that imposing equality between tensor train components to enforce *self-similarity* is not well justified if we do not

ensure that these components are written in the *same basis*. We overcome this obstacle by performing an extra *gauge fixing* optimization. This properly ensures *self-similarity*, while at the same time introducing little overhead. Compared to the previous algorithm of Ref. [GRK⁺20], gauge mediated weight sharing has significantly better numerical stability, run time and requires fewer random initialization. It allows us to recover laws for systems with 50 degrees of freedoms in a few minutes on desktop hardware. The underlying reason is that block-sparsity and self-similarity effectively reduce the polynomial degree of the objective function in the optimization problem while staying the physical corner.

The structure of this work is as follows. We first explain in Section 2 the various steps involved in limiting the ansatz class to the problem at hand. In Section 3, we then describe in detail our proposed *gauge mediated weight sharing* method. Section 4 then gives four examples of dynamical systems that are well suited for the proposed method and their specifics are discussed. We analyze three of these numerically in Section 5, demonstrating the effectivity and feasibility of the proposed approach in practice for ‘discovering dynamical laws from data’. Methods in this work are discussed for one-dimensional systems and tensor trains, however, we believe that they are generalizable to more dimensions using tensor networks containing loops, such as *projected entangled pair states* [CPGSV21, Oru14]. Some preliminaries of this are discussed in Section 4.

2 Finding the ansatz class for a specific problem

The SINDy algorithm identifies *sparse* dynamical laws with the goal of making the result interpretable. This is well motivated in the case of low d , when terms occurring on the right hand side of 1 have clear physical meaning. For many-body systems with large d though, this is not necessarily the case. Our proposal gives physically motivated ansatz class focusing on relevant features of the system. It is suitable for local, self-similar systems. We will now give the necessary steps to find this ansatz for a specific system.

The zeroth step is to identify the right coordinates $x \in \mathbb{R}^d$ to parametrize the state space. These should be chosen so that locality of the system is manifested in them. This means that they can be *ordered* in such a way that there is only negligible interaction between variables beyond some *interaction range*, which is independent of the system size. Note that this allows for some more exotic locality concepts, such as, e.g., locality in the momentum space. These variables should also give rise to sparse description of the system. Expert intuition is the most important resource here, although methods like *principle component analysis* (PCA) may be useful in some cases [CLKB19]. Given such a coordinate system with locality structure, we proceed in the following four steps that we will explain in detail in the remainder of the section.

1. Choose a suitable finite product basis.
2. Determine the block sparse structure.
3. Limit the block sizes (*low-rankness*).*
4. Choose the *selection map* for gauge mediated weight sharing (*self-similarity*).*

The steps labeled with an asterisk can potentially be automated using data, as discussed below.

2.1 Choosing the basis

By choosing a basis we mean identifying a suitable p -dimensional univariate *function dictionary*

$$\{\Psi_i : \mathbb{R} \rightarrow \mathbb{R}\}_{i=1}^p, \quad (4)$$

where Ψ_i are linearly independent. Potential choices are, e.g., monomials $x \mapsto \{1, x, x^2, \dots, x^{p-1}\}$, Legendre polynomials, Chebyshev polynomials, or trigonometric functions. Using these, we construct p^d multivariate basis functions

$$\phi_{i_1, \dots, i_d}(x) = \Psi_{i_1}(x^{(1)}) \dots \Psi_{i_d}(x^{(d)}), \quad (5)$$

where $i_\ell = 1, \dots, p$. This basis spans a finite dimensional subspace of the whole multivariate function space. Learning f is now reduced to finding coefficient tensors Θ_k , such that to a good approximation

$$f_k(x) \approx \sum_{i_1, \dots, i_d} \Theta_{k, i_1 \dots i_d} \phi_{i_1 \dots i_d}(x). \quad (6)$$

Expert knowledge is needed to choose the right dictionary and hence the right subspace, such that the relation Eq. (6) can be satisfied.

2.2 Block sparse structure

To parametrize the coefficient tensor $\Theta_{k, i_1, \dots, i_d}$ we use the tensor train decomposition [BSU16, BC17], which allows us to sharpen our ansatz towards the *physical corner* [ECP10] of local dynamical systems. The tensor train decomposition of the tensor $\theta_{k, i_1, \dots, i_D}$ can be written in *Penrose tensor network notation*¹ as

$$\Theta_{k, i_1, \dots, i_d} = \begin{array}{c} C_{k,1} \quad C_{k,2} \quad \dots \quad C_{k,d-1} \quad C_{k,d} \\ \bullet \quad \bullet \quad \dots \quad \bullet \quad \bullet \\ | \quad | \quad \dots \quad | \quad | \\ i_1 \quad i_2 \quad \dots \quad i_{d-1} \quad i_d \end{array} \quad (7)$$

This format can be achieved for any tensor $\Theta_{k, i_1, \dots, i_d}$ by repeated singular value decomposition (SVD) of the *matriciation* of the tensor, where one blocks the indices i_j for $j = 1, \dots, \ell$ and the remaining indices $i_{\tilde{j}}$ for $\tilde{j} = \ell + 1, \dots, d$ onto rows and columns of a matrix respectively, before performing (SVD) to create the link between $C_{k,\ell}$ and $C_{k,\ell+1}$.

¹In this notation, tensors are represented by nodes of a graph and indices by its edges. If two tensors are connected by an edge, they are contracted along the corresponding index.

For each k , the tensors $C_{k,\ell} \in \mathbb{R}^{r_{i-1} \times p \times r_i}$ are called the *tensor train components*. They carry a single physical index i_ℓ , which is called a *mode*, of dimension p and for $i = 2, \dots, d-1$ two virtual indices of dimensions r_{i-1} and r_i , which are contracted over to recover Θ_{k,i_1,\dots,i_d} . For $i = 1, d$ they have just one virtual index. The virtual dimensions (r_1, \dots, r_{d-1}) are called the *rank* of the tensor train. We can adjust the ansatz class to the problem at hand by varying the rank [DHZ⁺21]. Local dynamical systems can be well approximated by a low rank tensor train.² By *locality* we mean that the representation of f_k in the product basis chosen in Section 2.1 depends non-trivially only on variables x_i with $|i - k| < R$, where R is a d -independent *interaction range*. This is shown in *Theorem 5* of Ref. [GRK⁺20]. The locality does not need to be as strict though and good approximations can be obtained even for systems with decaying unbounded interactions, as shown by *Proposition 5.1* in Ref. [BSU16], discussed in Appendix A and demonstrated by our numerical examples in Section 5.

Given a function dictionary as in Section 2.1, we can reduce the number of parameters, simplify operations on the tensor train and further sharpen our ansatz class towards the *physical corner* by exploiting the unitary *gauge freedom*

$$\begin{array}{ccc}
\begin{array}{c} \bullet \\ | \\ C_{k,\ell} \\ | \\ \bullet \end{array} & \mapsto & \begin{array}{c} \bullet \\ | \\ C_{k,\ell} \\ | \\ \bullet \end{array} \begin{array}{c} \bullet \\ | \\ U \\ | \\ \bullet \end{array} \\
\begin{array}{c} \bullet \\ | \\ C_{k,\ell+1} \\ | \\ \bullet \end{array} & \mapsto & \begin{array}{c} \bullet \\ | \\ U^\dagger \\ | \\ \bullet \end{array} \begin{array}{c} \bullet \\ | \\ C_{k,\ell+1} \\ | \\ \bullet \end{array}
\end{array} \quad (8)$$

to put the tensor train into the *block sparse* format, as we now demonstrate. In the following discussion we restrict ourselves to the case where each physical index is assigned the same dictionary, but the discussion follows with little modification even for more complicated choices. The main idea here is to partition the values $i = 1, \dots, p$ of the physical index into groups and label them with a non-negative integer. This is a generalization of the concept of a polynomial degree, extended to other dictionaries. This defines a function $w : \{1, \dots, p\} \rightarrow \mathbb{N}_0$, which assigns each dictionary element a degree. We can use w to assign a degree also to each product basis element ϕ_{i_1,\dots,i_d} by

$$\tilde{w}(i_1, \dots, i_d) := \sum_{j=1}^d w(i_j). \quad (9)$$

We can use this to define the Laplace-like operator

$$L = \sum_{j=1}^d \text{Id}_p \otimes \dots \otimes \text{diag}(w(1), \dots, w(p)) \otimes \dots \otimes \text{Id}_p, \quad (10)$$

which satisfies $L\phi_{i_1,\dots,i_d} = \tilde{w}(i_1, \dots, i_d)\phi_{i_1,\dots,i_d}$ and hence counts the degree of a function in the span of the product basis by acting on its coefficient tensor.

²What is really meant here is that the rank of the tensor train is independent of d . This is equivalent to the area law scaling of entropy in quantum many body systems. For a discussion of this connection, see Appendix A.

Suppose for a moment that we have a tensor train representation Θ_k (where we are suppressing the physical indices) of a function f_k , which is an eigenvector of L with eigenvalue μ . Consider the virtual index connection in Equation 7 between $C_{k,\ell}$ and $C_{k,\ell+1}$, which we will call the *interface* at ℓ . By splitting the tensor train at this interface, we obtain the the *left interface vector*

$$\tau_{\ell,m,i_1,\dots,i_\ell}^{\leq}(\Theta_k) = \begin{array}{c} C_{k,1} \quad C_{k,2} \quad \dots \quad C_{k,\ell} \\ | \quad | \quad \dots \quad | \\ i_1 \quad i_2 \quad \dots \quad i_\ell \end{array} m \quad (11)$$

and the *right interface vector*

$$\tau_{\ell+1,m,i_{\ell+1},\dots,i_d}^{\geq}(\Theta_k) = m \begin{array}{c} C_{k,\ell+1} \quad \dots \quad C_{k,d} \\ | \quad \dots \quad | \\ i_{\ell+1} \quad \dots \quad i_d \end{array}. \quad (12)$$

In general, for a given choice of index m , the interface vectors will not have a well defined degree. However, by exploiting the *gauge freedom* Eq. (8), we can always find a unitary U , such that we can assign to the resulting tensor train a well defined degree. This means that $\tau_{\ell,m}^{\leq}$ and $\tau_{\ell+1,m}^{\geq}$ will become eigenvectors of the partial operators $L_\ell^{\leq} : \mathbb{R}^{p^\ell} \rightarrow \mathbb{R}^{p^\ell}$ and $L_\ell^{\geq} : \mathbb{R}^{p^{d-\ell}} \rightarrow \mathbb{R}^{p^{d-\ell}}$ defined by

$$\begin{aligned}
L_\ell^{\leq} &= \sum_{j=1}^{\ell} \text{Id}_p \otimes \dots \otimes \text{diag}(w(1), \dots, w(p)) \otimes \dots \otimes \text{Id}_p, \\
L_{\ell+1}^{\geq} &= \sum_{j=\ell+1}^d \text{Id}_p \otimes \dots \otimes \text{diag}(w(1), \dots, w(p)) \otimes \dots \otimes \text{Id}_p.
\end{aligned} \quad (13)$$

Suppose we follow this procedure for all $\ell = 1, \dots, d-1$. Consider now the component $C_{k,\ell}$ and write the matrix corresponding to the physical index i as ${}^i M^{k,\ell}$. Let μ_m and μ_n be the eigenvalues of $\tau_{\ell-1,m}^{\leq}$ and $\tau_{\ell+1,n}^{\geq}$ respectively. Because Θ_k is an eigenvector of L with eigenvalue μ , the element $({}^i M^{k,\ell})_{m,n}$ will be identically zero whenever $\mu_m + \mu_n + w(i) \neq \mu$. This leads to block sparsity of the tensor train components.

Block sparsity is particularly familiar in the case of a monomial dictionary, which is the example discussed in Ref. [GST21]. In this case let $w(i) = i - 1$, so that the operator L and its partial operators count the polynomial degree. This is analogous to the particle number operator in quantum physics. The block sparse structure of the components for $p = 4$ and degree 3 monomial tensor train now

becomes

$$\begin{aligned}
{}^0 M^{k,\ell} &= \begin{pmatrix} * & 0 & 0 & 0 \\ 0 & * & 0 & 0 \\ 0 & 0 & * & 0 \\ 0 & 0 & 0 & * \end{pmatrix}, \\
{}^1 M^{k,\ell} &= \begin{pmatrix} 0 & * & 0 & 0 \\ 0 & 0 & * & 0 \\ 0 & 0 & 0 & * \\ 0 & 0 & 0 & 0 \end{pmatrix}, \\
{}^2 M^{k,\ell} &= \begin{pmatrix} 0 & 0 & * & 0 \\ 0 & 0 & 0 & * \\ 0 & 0 & 0 & 0 \\ 0 & 0 & 0 & 0 \end{pmatrix}, \\
{}^0 M^{k,\ell} &= \begin{pmatrix} 0 & 0 & 0 & * \\ 0 & 0 & 0 & 0 \\ 0 & 0 & 0 & 0 \\ 0 & 0 & 0 & 0 \end{pmatrix},
\end{aligned} \tag{14}$$

This can be straightforwardly extended to Legendre polynomials.

In this work, we will also need trigonometric dictionary, which needs a slight adjustment of the block sparse structure. E.g., for $p = 3$ and dictionary $x \mapsto (1, \sin x, \cos x)$, we have chosen $w(1) = 0$, $w(2) = w(3) = 1$, so that the eigenvalue counts the number of sines and cosines, which can be coined trigonometric degree. Now for trigonometric degree 2 the block sparse structure becomes

$$\begin{aligned}
{}^0 M^{k,\ell} &= \begin{pmatrix} * & 0 & 0 \\ 0 & * & 0 \\ 0 & 0 & * \end{pmatrix}, \quad {}^1 M^{k,\ell} = \begin{pmatrix} 0 & * & 0 \\ 0 & 0 & * \\ 0 & 0 & 0 \end{pmatrix}, \\
{}^2 M^{k,\ell} &= \begin{pmatrix} 0 & * & 0 \\ 0 & 0 & * \\ 0 & 0 & 0 \end{pmatrix}.
\end{aligned} \tag{15}$$

To extend the ansatz class beyond eigenvectors of L while preserving block sparsity, we can use *sums* of eigenvectors of L with eigenvalues $\leq \mu$. We do this by introducing an extra tensor train component $C_{k,d+1} = \text{Id}_\nu$ with a dictionary $\Psi_{d+1} = (1, \dots, 1)$ of dimension equal to the number ν of eigenspaces we wish to include. The resultant tensor train becomes

$$\Theta_{k,i_1,\dots,i_d} = \begin{array}{ccccccc}
C_{k,1} & C_{k,2} & & \dots & & C_{k,d} & \text{Id}_\nu \\
\bullet & \bullet & & & & \bullet & \bullet \\
| & | & & & & | & | \\
i_1 & i_2 & & & & i_d & \Psi_{d+1}
\end{array} \tag{16}$$

where the final component just sums over the terms with different eigenvectors. Limiting the degree of the ansatz class in this way can be in many cases well physically justified. For example in the case of monomial dictionary we get polynomials of degree bounded by μ . This is advantageous because most functions in nature can be approximated by low degree polynomials and because this restriction makes our ansatz class numerically much better behaved, leading to huge improvements over plain SINDy.

2.3 Limiting the block size

In case of block sparse tensor trains limiting the rank amounts to limiting the *block sizes*. The maximum rank for each mode of a block sparse tensor train is the sum of its block sizes. Ref. [GST21, Lemma 3.3] gives bounds on these in the case of full-rank tensor trains, which are strongly d -dependent, manifesting the curse of dimensionality. However, as discussed in the previous section, if the system has approximate d -independent *locality*, it can be well-approximated by a tensor train with d -independent rank. Therefore, also the block sizes have d -independent bounds. See Ref. [GST21, Theorem 3.4] for a formal prove for monomial bases and strict locality. For further discussion on approximate locality, we refer to [BSU16] and Appendix A. Given a maximum block size, we then choose for the size of a specific block $\max(\text{maximum block size}, d \text{ dependent general bound})$.

The block sizes can be tuned until desired accuracy of the approximation Eq. (6) is achieved. This process can also be automated by using rank adaptive methods, such as *SALSA* [GK19]. However, in this work, we refrain from doing so and use plain *alternating least squares* (ALS) optimization. Notice that using higher rank approximations increases the number of samples needed in order to achieve the desired accuracy. This can be seen in the numerical experiments in Section 5.

2.4 Choosing the selection map

The final decision we need to make before turning the handle and learning the system, is to choose the *selection map*. In many systems, structural similarities between equations allow us to reuse the same tensor train component in multiple equations, which is a principle we call *self-similarity*. This reduces the number of parameters to be learned, while also potentially making the method more robust against noise in the data, since it allows us to use data of multiple equations to learn a single component. This is the basis of *gauge mediated weight sharing*, our algorithmic approach detailed in Section 3. First, we need to choose n , the number of distinct components per mode that are required. This means that we need components $\tilde{C}_{\tilde{k},\ell}$ for $\tilde{k} = 1, \dots, n$ and $\ell = 1, \dots, d$ and an extra component $\tilde{C}_{1,d+1} = \text{Id}_\nu$ due to block sparsity, as described in Section 2.2.

The *selection map* $S \in \mathbb{R}^{d \times (d+1)}$ then has elements $S_{i,j} \in \{1, \dots, n\}$, which determine the precise way, in which the components are reused

$$C_{k,\ell} = \tilde{C}_{S_{k,\ell},\ell}. \tag{17}$$

Note that we need $S_{k,d+1} = 1$ for all k . As an illustration, let us give a concrete example. Consider a $d = 6$ system with $n = 3$. This means that the unique components that

are needed to describe such a system are

$$(18)$$

There is also the order 2 component $\tilde{C}_{1,7} = \text{Id}_\nu$, which is due to block sparsity and where ν gives the number of eigenspaces of L we wish to include. This component is not learned and is determined by the block sparse structure. Now let the block sparse tensor train representations of all the equations be

$$(19)$$

This structure is compactly captured by the *selection map*

$$S = \begin{pmatrix} 2 & 1 & 1 & 1 & 1 & 1 & 1 \\ 3 & 2 & 1 & 1 & 1 & 1 & 1 \\ 3 & 3 & 2 & 1 & 1 & 1 & 1 \\ 3 & 3 & 3 & 2 & 1 & 1 & 1 \\ 3 & 3 & 3 & 3 & 2 & 1 & 1 \\ 3 & 3 & 3 & 3 & 3 & 2 & 1 \end{pmatrix}. \quad (20)$$

The precise form of the selection map has to be chosen by and large based on expert intuition. In this work, all examples have the same kind of *selection map*, which takes the form

$$S = \begin{pmatrix} \tilde{n} & \tilde{n}-1 & \dots & 2 & 1 & 1 & \dots & 1 & 1 \\ \tilde{n}+1 & \tilde{n} & \tilde{n}-1 & \dots & 2 & 1 & \dots & 1 & 1 \\ n & \dots & n & n-1 & \dots & 1 & \dots & 1 & 1 \\ n & \dots & n & n-1 & \dots & \tilde{n} & \tilde{n}-1 & 1 & 1 \\ n & \dots & n & n-1 & \dots & \tilde{n}+1 & \tilde{n} & 1 & 1 \end{pmatrix}, \quad (21)$$

where $\tilde{n} = \lceil n/2 \rceil$ is on the diagonal of each row. Physically, this means that the k th mode interacts strongly only with modes, which are not too far in the locality order. The rest of the interactions are combined into a single effective component. In this case, we call n the *interaction range*. Now it is possible to learn n from the data, however, in our numerical examples we do not exploit this option.

3 Alternating least-square optimization with gauge-mediated weight sharing

Here we describe in detail the new method of *weight-sharing* used to utilize *self-similarity*. This proposal replaces the usage of an explicit *selection tensor* in Ref. [GRK⁺20], which has turned out to be numerically badly conditioned for higher orders (i.e., $d > 20$). This issue did not become apparent in the previous work, since systems up to only $d = 18$ were considered. The problem with the *selection tensor* approach is that it does not properly take into account the *gauge freedom*, neglecting the fact that each equation has its own *gauge condition*, as elaborated on below. Both of these approaches use the ALS algorithm. While the previous approach solves in each sweep n optimization problems per mode, *gauge mediated weight sharing* solves $O(n^2)$ optimizations per mode in each sweep in the worst case. However, as shown in Section 5 and justified theoretically in this section, *gauge mediated weight sharing* leads to much better numerical conditioning of the algorithm. In the following, we have chosen to perform the ALS sweeps from left to right.

Tensor train components of the same mode, which have equal corresponding entries in the selection map (see Section 2.4), i.e., with $S_{\ell,k} = S_{\tilde{\ell},k}$, are of the ‘‘same type’’. This alone however, does not guarantee that they really have equal entries, because they can be written in different bases. The choice of these bases is determined by their left neighbouring component (i.e., by $C_{S_{\ell,k-1},k-1}$ and $C_{S_{\tilde{\ell},k-1},k-1}$, which can be different) and is completely arbitrary, because of the unitary³ *gauge freedom* left after orthogonalization in the previous ALS step. The *gauge mediated weight sharing* approach fixes this unitary *gauge freedom* to ensure that components of the same type really do have equal entries. We do this by optimizing a given component based only on data of equations in which the left neighbour is equal. The newly found component is then used in the remaining equations, where we perform an extra optimization to find the basis transformation to the basis, in which this component is written. The formal steps are given in Algorithm 1 and we further illustrate it below by going explicitly through one ALS step.

Consider optimizing the 4th mode in the system described by Eq. (19). I.e., we intend to optimize the components $C_{2,4}$, $C_{1,4}$ and $C_{3,4}$. Since $C_{1,4}$ is only used once, it can be optimized as usual using available data of the fourth equation. The component $C_{3,4}$ is used in the fifth and sixth equation, but its left neighbours are $C_{3,3}$ in both equations. These have equal entries, as ensured by *gauge mediated weight sharing* in the previous ALS step. Therefore, we can optimize $C_{3,4}$ using data of the fifth and sixth equations together. The component $C_{2,4}$ is problematic, since it has different left neighbours in the equations where it occurs. We use data from just the first two equations to optimize it, which we can do since $S_{1,3} = S_{2,3} = 3$. However, in

³In this work, we are only working with real tensor trains, so this reduces to orthogonal freedom.

Algorithm 1: Calculation of tensor train components to recover the dynamical system.

input : Data pairs $(x_i, y_i) \in \mathbb{R}^d \times \mathbb{R}^d, i = 1, \dots, M$,
maximal number of sweeps $maxSweeps$,
number of different components per mode n ,
Selection Matrix S , maximum block size m

output : nd Block sparse tensor train components.

For $k = 1, \dots, d, \ell = 1, \dots, n$ initialize block sparse $C_{\ell,k}$ with maximum block size m ;

```

for  $j = 1, \dots, maxSweeps$  do
  for  $k = 1, \dots, d$  do
    for  $\ell = 1, \dots, n$  do
      if  $C_{\ell,k}$  is used only once then
        Optimize component  $C_{\ell,k}$ ;
      end
      else
        Let  $eqs$  be the indices of the equations
        where  $C_{\ell,k}$  is used;
        Divide  $eqs$  into sets  $E_i$  for
         $i = 1, \dots, m$  according to the value
        of  $S_{ek-1}$  for  $e \in eqs$  and sort them
        so that  $|E_i| \geq |E_j|$  for  $i < j$ .;
        Optimize component  $C_{\ell,k}$  using the
        data of all  $e \in E_1$ ;
        for  $i = 2, \dots, m$  do
          With the updated  $C_{\ell,k}$ , use the data
          of all equations in  $E_i$  to find the
          optimal  $U_i$  according to Eq. (22);
          Update  $C_{S_{ik-1}k-1}$  using  $U_i$ 
          according to Eq. (23);
        end
      end
    end
  end
  if termination criterion is met then
    break;
  end
end
return  $C_{k,\ell}, k = 1, \dots, d, \ell = 1, \dots, n$ .

```

the third equation $S_{3,4} \neq 3$, so here we may need a change of basis before we can use the newly found $C_{2,4}$ as it is. To find the correct change of basis, we look for an (ideally orthogonal⁴) matrix U minimizing the least square error of the third equation data with

$$\begin{array}{cccccccc} C_{3,1} & C_{3,2} & C_{1,3} & U & C_{2,4} & C_{2,5} & C_{2,6} & C_{2,7} \\ \bullet & \bullet & \bullet & \bullet & \bullet & \bullet & \bullet & \bullet \\ | & | & | & | & | & | & | & | \\ \hline \end{array}, \quad (22)$$

⁴This matrix will be orthogonal in theory, but our code performs optimization over all matrices to find it. Using optimization over the orthogonal group is possible and could potentially improve numerical stability.

where the newly found component $C_{2,4}$ is used. We then update $C_{1,3}$ to

$$\begin{array}{ccc} C_{1,3} & U & \\ \bullet & \bullet & \\ | & | & \\ \hline \end{array}. \quad (23)$$

This idea of backward correction of the basis is methodically similar to the algorithm in Ref. [HLO⁺16] for solving the time-dependent Schrödinger equation using the *time-dependent variational principle* (TDVP).

4 Example systems and discussion

In this section we will introduce four examples of dynamical systems, which are well suited for our method. The starting point in Ref. [GRK⁺20] has been the *Fermi-Pasta-Ulam-Tsingou* (FPUT) system, described by

$$\begin{aligned} f_k(x) = & \kappa_{k+1}(x_{k+1} - x_k) - \kappa_k(x_k - x_{k-1}) \\ & + \beta_{k+1}(x_{k+1} - x_k)^3 - \beta_k(x_k - x_{k-1})^3 \quad (24) \\ & k = 1, \dots, d, \end{aligned}$$

where we allow for the different springs to have different spring constants κ_k and different non-linearity constants β_k . This is a dynamical system, where each equation can be exactly represented by a tensor train of rank at most 4, for polynomial dictionary of degree at least 3. Hence we can choose the monomial function dictionary with $p = 4$, with block sparsity given in Section 2.2. We can limit the rank to 4 independent of d . *Self-similarity* can be easily seen from $f_k(x) = \tilde{f}(x_{k-1}, x_k, x_{k+1})$, which means that we can choose $n = 5$ for any d to represent the system exactly. This concludes the first and simplest example. In Section 5 we give numerical evidence showing that with *gauge mediated weight sharing* we can model systems of sizes > 20 .

The second example is a model of classical magnetic dipoles along a 1-dimensional line, which are free to rotate in the plane perpendicular to it. This system is given by

$$f_k(x) = I_k M_k \sum_{\ell \neq k} \frac{M_\ell}{|X_k - X_\ell|^3} \sin(x_k - x_\ell), \quad (25)$$

where I_k, M_k and X_k are the moment of inertia, magnetic dipole moment and position along the line of the k th dipole respectively. The X 's should be chosen so that $X_1 < X_2 < \dots < X_d$, which ensures that the dynamical system admits a local structure and hence can be well approximated by a low rank tensor train. For our experiments, we have chosen the dipoles to be identical and equally separated, i.e., $I_k = I = 1, M_k = M = 1, X_k = sk$ for all $k = 1, \dots, d$. The distance s controls the locality of the system and can be tuned to ensure that it can be well approximated by a low rank tensor train. Structural similarity and decaying interaction implies *self-similarity* as specified at the end of Section 2.4 with *interaction range* $n < d$ (n is independent of d). In Section 5 we give numerical evidence for different p, n and d , showing that this is indeed the case. An important point to make for

this example is the *choice of basis*. While $\sin(x)$ can be well approximated by odd polynomials on the interval $[-\pi, \pi]$ using Taylor’s theorem, we already need degrees 7 or higher to recover the system up to relative error of order $1e-3$. Due to the trigonometric identities one can also use much smaller dictionaries of trigonometric functions. As discussed in Section 2.2, we have to use an appropriate *block sparse* structure, which differs slightly from the polynomial case. This system can be exactly described using dictionary $(1, \sin x, \cos x)$.

As a third example we will look at a one dimensional chain of atoms, interacting via a modified *Lennard-Jones potential*. The system is given by

$$f_k(x) = 6m_k \sum_{\ell \neq k} \text{sign}(x_k - x_\ell) \frac{\varepsilon_{k,\ell}}{\sigma_{k,\ell}} \left(2 \left(\frac{\sigma_{k,\ell}}{|x_k - x_\ell|} \right)^{2q+1} - \left(\frac{\sigma_{k,\ell}}{|x_k - x_\ell|} \right)^{q+1} \right), \quad (26)$$

where $q = 6$ for the standard Lennard-Jones. Here M_k is the mass of the k th atom and $\sigma_{k,\ell}, \varepsilon_{k,\ell}$ are parameters of the interaction between the k th and l th atom, which need to be symmetric, $\sigma_{k,\ell} = \sigma_{\ell,k}, \varepsilon_{k,\ell} = \varepsilon_{\ell,k}$. In particular, $\varepsilon_{k,\ell}$ controls the depth of the potential and $\sigma_{k,\ell}$ the equilibrium distance. Notice that we can remove the sign function and the absolute values for even q , which is beneficial to the learning. High inverse powers are hard to learn using polynomial bases on an ordinary personal computer, so we only use $q = 2$ for our numerical examples. Our experiments use the case where $\varepsilon_{k,\ell} = \sigma_{k,\ell} = m_k = 1$. To deal with the problematic divergence at vanishing separation, instead of the function f itself we learn

$$g_k(x) = (x_k - x_{k-1})^{2q+1} (x_k - x_{k+1})^{2q+1} f_k(x), \quad (27)$$

which improves the numerical performance. This is inspired by the approach suggested in Ref. [MBPK16] for learning rational functions. Some care needs to be taken when drawing the initial conditions of this model, so that the atoms do not fly off to infinity. Besides working in the zero momentum frame, we have to limit the amount of energy in the system, which is given by

$$E = \sum_{k < \ell} \varepsilon_{k,\ell} \left[\left(\frac{\sigma_{k,\ell}}{|x_k(0) - x_\ell(0)|} \right)^{2q} - \left(\frac{\sigma_{k,\ell}}{|x_k(0) - x_\ell(0)|} \right)^q \right] + \sum_k \frac{1}{2} m_k \dot{x}_k^2(0). \quad (28)$$

The restriction $E < 0$ prevents all atoms from separating and is the obvious first step, but it can still happen that atoms separate into clusters that fly off. Limiting $E < -(d-2)/4$ prevents this from happening, but it is too restrictive to be practical. Better bounds are difficult to find. We have chosen a monomial basis for this model. Decaying interaction allows us to use a low rank representation and limit the *interaction range* n in this system just as in the case of magnetic dipoles. This model is, however, substantially harder to learn, since this time locality varies

dynamically. On the other hand ordering of the particles does not change, because the potential is infinite at zero separation. If the positions x are ordered initially, one can therefore still expect to learn this model efficiently.

The final example is a chain of massive particles interacting via gravitational potential. This system is described by

$$f_k(x) = -Gm_k \sum_{\ell \neq k} \frac{m_\ell}{|x_k - x_\ell|^2} \text{sign}(x_k - x_\ell), \quad (29)$$

where m_k are masses of the particles and G the gravitational constant. This example is very similar to the previous one, however, the potential is bounded from above at zero separation, so the ordering of the particles will change in time, varying the locality structure dynamically. This makes learning of this model even more difficult. To proceed, we suggest to use tensor trains with different ordering of the variables for each configuration. One now learns each of these using data that correspond to configurations with the correct ordering. To limit the computational effort required, one should only learn the orderings that are of practical interest. We do not explore this method further in this work.

Although, we only discussed one dimensional dynamical systems, which can be captured well by tensor trains, we believe that these ideas can be extended to 2 and 3 dimensional dynamics using tensor networks containing loops. Here one deals in many cases with variable switching as in the last example. Our proposed method for dealing with this difficulty can be utilized here.

5 Numerical experiments

To numerically test our method, we slightly simplified the setting. Instead of simulating the actual dynamics, computing \dot{x} or \ddot{x} from data and using these values to learn f , we sample randomly from the function f subject to some conditions on the sample points determined by the system. For example, while for the magnetic dipole system we can draw any $x \in [0, 2\pi]^d$, the Lennard-Jones example requires that $x_1 < \dots < x_d$ and also that $a \leq x_i - x_{i-1} \leq b$ for all $i = 2, \dots, d$ and carefully chosen positive constants a, b . The second condition comes from conservation of energy, where if there is not too much energy in the system initially, its dynamics would never explore states violating this condition.

The experiments are initiated with a random tensor train and trained using Algorithm 1 on a varying number of samples. The model is then benchmarked against the true functions f evaluated at 2×10^4 random samples, drawn subject to the conditions mentioned above. We calculate the residuum using the relative ℓ^2 -norm $\|\tilde{f}(x) - f(x)\|_2 / \|f(x)\|_2$, where $\tilde{f}(x)$ is the vector of model evaluations on the testing points and $f(x)$ the vector of true values on these points. The residuum is then used to evaluate the success of the recovery.

We have performed numerical experiments on the FPUT system, magnetic dipoles and modified Lennard-Jones.

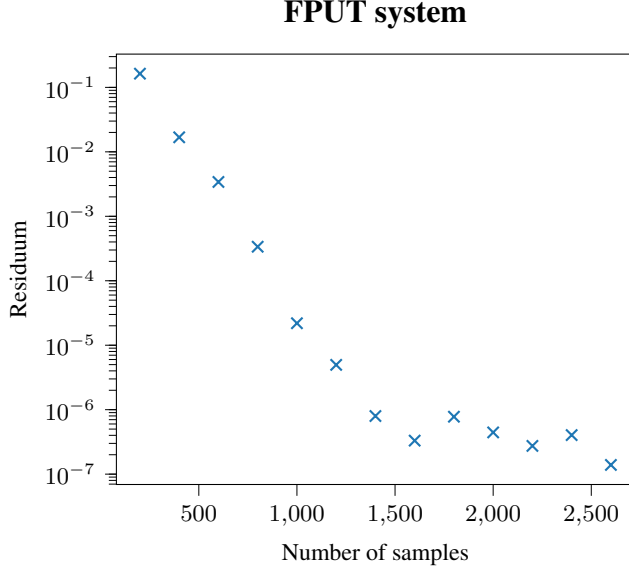


Figure 1: Recovery of a 50 particle FPUT system with identical non-linear springs with $\kappa_k = 1$, $\beta_k = 0.7$. We use Legendre polynomial dictionary of degree 3, maximum block size 2 and interaction range $n = 5$. The maximum number of sweeps has been set to 10.

All of the experiments were performed on an ordinary household computer and the code has not been optimized for speed. Therefore it serves mainly as a proof of concept, showcasing the capabilities of the suggested approach.

In Fig. 1, we display the results for the FPUT system Equation 24, where we have chosen $\kappa_k = 1$ and $\beta_k = 0.7$. The figure shows recovery of a system of $d = 50$ particles, demonstrating the improvement *gauge mediated weight sharing* gives over the previous method of *selection tensor* used in Ref. [GRK⁺20], which showed severe numerical issues for systems with ~ 20 particles. We used degree 3 Legendre polynomials dictionary, interaction range $n = 5$ selection map, maximum block size of 2 and maximum number of ALS sweeps 10. The figure demonstrates recovery of this system, achieving residua of the order 5×10^{-7} when training on at least 1400 sample points.

We have also performed an experiment on the FPUT system with varying κ_k , which we have chosen from a uniform distribution on $[0, 2]$, and β_k , which we have drawn from the uniform distribution on $[0, 1.4]$. This choice has been made so that the two experiments on the FPUT system both have the same expectation value of the parameters. Fig. 2 shows similar recovery to the symmetric case, but here we require at least 1800 samples, demonstrating that this system is slightly harder to learn.

The main part of the experiment has been performed on the chain of magnetic dipoles given by Eq. (25). For all the following experiments we set the maximum number of ALS sweeps to 8 and maximum block size to 3. We demonstrate the recovery abilities of our method on systems of

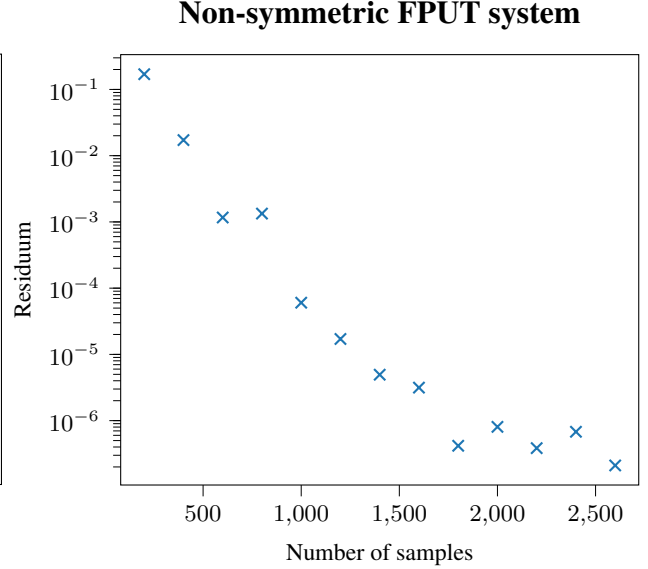


Figure 2: Recovery of the 50 particle FPUT system with varying spring constant κ_k , chosen from the uniform distribution on $[0, 2]$ and non-linearity coefficient β_k , chosen from the uniform distribution on $[0, 1.4]$. We use Legendre polynomial dictionary of degree 3, maximum block size $m = 3$, interaction range $n = 5$ and maximum number of sweeps 10.

varying size between $d = 10$ and $d = 50$ dipoles, with interaction ranges $n = 5$ and $n = 9$. In Fig. 3 we use a trigonometric dictionary $\{1, \sin x, \cos x\}$ and demonstrate recovery down to residua of 1.5×10^{-3} for $n = 5$ and 1.5×10^{-4} for $n = 9$. We can see how the number of samples required for recovery with increases with the size of the system.

Fig. 4 shows a similar experiment, but now using Legendre polynomials of degree 9 instead of the trigonometric dictionary. We were able to achieve residuum of 3×10^{-3} , but we required about 30 times more samples to recover a $d = 30$ system than when using trigonometric dictionary, while obtaining a larger residuum.

Robustness of the method against noise is demonstrated in Fig. 5. We corrupted the learning data with additive unbiased Gaussian noise with standard deviation $\sigma = 0.1, 0.01, 0.001$. In this case we plot the residuum averaged over 5 different runs.⁵ Trigonometric dictionary has been used and we demonstrate the ability to recover a chain of $d = 50$ dipoles to residuum about 3×10^{-2} for $\sigma = 0.1$ and 10^{-3} for $\sigma = 10^{-3}$.

The final experiment has been performed on the modified Lennard-Jones system Eq. (27) with $q = 2$. The results are plotted in Fig. 6. This system is significantly harder to recover, as demonstrated by the outliers in recovery.

⁵Each run has newly drawn learning data and a newly initiated tensor train.

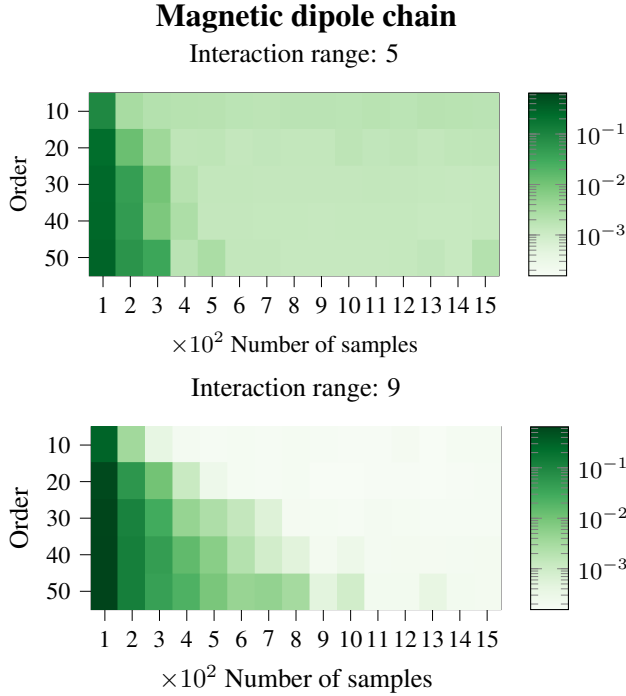


Figure 3: Recovery of the magnetic dipoles chain using trigonometric dictionary $\{1, \sin x, \cos x\}$ for varying sizes of system and interaction ranges. The shading displays the ℓ_2 residuum after recovery against 2×10^4 random samples. Maximum number of sweeps has been set to 8 and maximum block size 3.

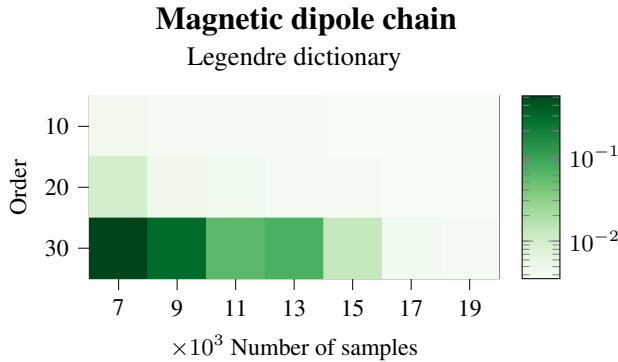


Figure 4: Recovery of the magnetic dipoles chain with the dictionary of Legendre polynomials degree 9. The shading displays the ℓ_2 residuum after recovery against 2×10^4 random samples. We can see a significantly worse recovery than using the trigonometric dictionary. Maximum number of sweeps has been set to 8, maximum block size to 3 and interaction range to $n = 5$.

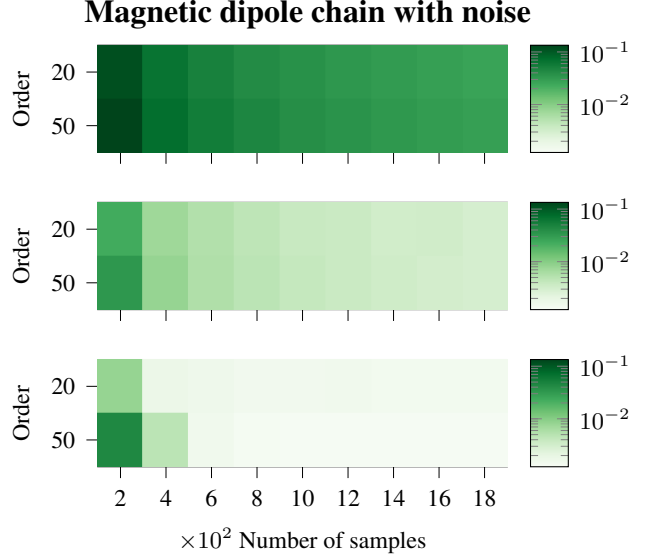


Figure 5: Magnetic dipoles with additive Gaussian noise with standard deviation σ , trigonometric dictionary. The top plot is for $\sigma = 0.1$, the middle plot for $\sigma = 0.01$ and the bottom plot for $\sigma = 0.001$. The shading displays the ℓ_2 residuum after recovery against 2×10^4 random samples.

This is because the Lennard-Jones potential is not easily expressible in polynomial bases and also because the locality varies dynamically. Nonetheless, we demonstrate the ability to recover a system of $d = 10$ particles down to residuum of about 1.5×10^{-2} using 7000 samples. We set the interaction range to $n = 5$, maximum number of sweeps to 8 and Legendre polynomials of degree 8 have been used.

We compare the performance when using varying maximum block sizes. The figure clearly shows that higher rank tensor trains are more expressive (achieve lower final residuum), but require more data to learn. The outliers signalize that this problem is not as well numerically conditioned as the previous examples. This can be also seen from the fact that a given ALS sweep occasionally leads to an increase in the training residuum, before decreasing again towards a different minimum. Hence we observed an improvement when we removed residuum increase from the stopping criteria and only relied on the specified maximum number of sweeps.

6 Conclusions

In this work, we have proposed a new method for recovering dynamical systems from data using tensor networks, extending the SINDy algorithm [BPK16]. Our method uses block sparsity [GST21] and a new approach to self-similarity, which we call *gauge mediated weight sharing*, instead of the *selection tensor* approach used in Ref. [GRK⁺20]. *Gauge mediated weight sharing* exploits the unitary *gauge freedom* of the tensor train decomposi-

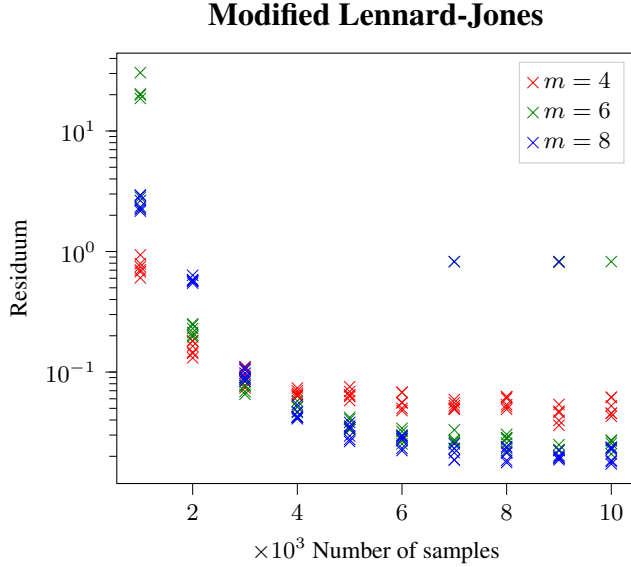


Figure 6: Recovery of the modified ($q = 2$) Lennard-Jones system of size $d = 10$, using the dictionary of degree 8 Legendre polynomials with interaction range $n = 5$, maximum number of sweeps 8 and varying maximum block size m given by the colour coding. Notice the three outliers resulting from the difficulty of recovering this system.

tion to properly fix the basis of tensor train components of the same type. We described how to limit the ansatz class of a given system to the *physical corner*, before it can be recovered from data. We suggest how to automate this process to some extent. Otherwise expert intuition is needed that specifies meaningful hypothesis classes.

The way the function dictionaries incorporate locality, the resulting dynamical laws found remain *interpretable*: The right hand sides of the differential equations governing the dynamics take a simple form in terms of powers of derivatives that can be physically interpreted as resulting from meaningful interactions.

Numerical evidence for the performance of the method is given for the *Fermi-Pasta-Ulam-Tsingou* (FPUT) equations, chain of magnetic dipoles and a chain of particles interacting via the modified Lennard-Jones potential. For the first two examples we demonstrate the ability of the method to recover the system of up to 50 particles. We recover the FPUT system down to residuum of 5×10^{-7} and the magnetic dipole chain to residuum 1.5×10^{-4} . Robustness of the method against noise is demonstrated in the magnetic dipole system and recovery down to noise level is achieved. We also show the performance of the algorithm when recovering a significantly more demanding system of modified Lennard-Jones interacting particles. Here we show recovery of a 10 particle system to residuum 1.5×10^{-2} . Our work hints on ways of generalizing our method to systems with more than one dimension and to systems where the order of particles changes dynamically.

It is the hope that this work substantially contributes to the growing body of literature displaying in what versatile fashion tensor networks can be used in settings beyond capturing quantum many-body systems, specifically in the context of learning tasks and in probabilistic modelling [IMW⁺20, GSP⁺19, SS16, KG19, GPA⁺18].

7 Acknowledgements

We thanks A. Goeßmann and R. Schneider for insightful discussions. This work has been funded by the DFG (Interdisciplinary Research Training Group DAEDALUS RTG 2433 and EI 519/15-1) and the Cluster of Excellence MATH+.

References

- [BC17] J. C. Bridgeman and C. T. Chubb. Hand-waving and interpretive dance: An introductory course on tensor networks. *Journal of Physics A*, 50:223001, 2017.
- [BGP21] M. Bachmayr, M. Götte, and M. Pfeffer. Particle number conservation and block structures in matrix product states. 2021. arXiv:2104.13483.
- [BPK16] S. L. Brunton, J. L. Proctor, and J. N. Kutz. Discovering governing equations from data by sparse identification of nonlinear dynamical systems. *Proceedings of the National Academy of Sciences*, 113:3932–3937, 2016.
- [BSU16] M. Bachmayr, R. Schneider, and A. Uschmajew. Tensor networks and hierarchical tensors for the solution of high-dimensional partial differential equations. *Foundations of Computational Mathematics*, 16:1423–1472, 2016.
- [CDA⁺21] C. Cornelio, S. Dash, V. Austel, T. R. Josephson, J. Goncalves, K. L. Clarkson, N. Megiddo, B. El Khadir, and L. Horesh. AI Descartes: Combining data and theory for derivable scientific discovery. 2021. arXiv:2109.01634.
- [CLKB19] K. Champion, B. Lusch, J. N. Kutz, and S. L. Brunton. Data-driven discovery of coordinates and governing equations. *Proceedings of the National Academy of Sciences*, 116:22445–22451, 2019.
- [CPGSV21] J. I. Cirac, D. Pérez-García, N. Schuch, and F. Verstraete. Matrix product states and projected entangled pair states: Concepts, symmetries, theorems. *Reviews of Modern Physics*, 93:045003, 2021.
- [CPSW21] A. Carderera, S. Pokutta, C. Schütte, and M. Weiser. CINDy: Conditional gradient-based Identification of Non-linear

- Dynamics – Noise-robust recovery. 2021. arXiv:2101.02630.
- [CSS15] N. Cohen, O. Sharir, and A. Shashua. On the expressive power of deep learning: A tensor analysis. 2015. arXiv:1509.05009.
- [DHZ⁺21] M. Ding, T.-Z. Huang, X.-L. Zhao, M. K. Ng, and T.-H. Ma. Tensor train rank minimization with nonlocal self-similarity for tensor completion. *Inverse Problems and Imaging*, 15:475–498, 2021.
- [dSCQ⁺20] B. M. de Silva, K. Champion, M. Quade, J.-C. Loiseau, J. N. Kutz, and S. L. Brunton. PySINDy: A Python package for the sparse identification of nonlinear dynamics from data. 2020. arXiv:2004.08424.
- [ECP10] J. Eisert, M. Cramer, and M. B. Plenio. Colloquium: Area laws for the entanglement entropy. *Reviews of Modern Physics*, 82:277–306, 2010.
- [GGR⁺20] A. Goeßmann, M. Götte, I. Roth, R. Sweke, G. Kutyniok, and J. Eisert. Tensor network approaches for learning non-linear dynamical laws. 2020. arXiv: 2002.12388.
- [GK19] L. Grasedyck and S. Krämer. Stable ALS approximation in the TT-format for rank-adaptive tensor completion. *Numerische Mathematik*, 143:855–904, 2019.
- [GKES19] P. Gelß, S. Klus, J. Eisert, and C. Schütte. Multidimensional approximation of nonlinear dynamical systems. *Journal of Computational and Nonlinear Dynamics*, 14, 2019.
- [GPA⁺18] I. Glasser, N. Pancotti, M. August, I. D. Rodriguez, and J. I. Cirac. Neural-network quantum states, string-bond states, and chiral topological states. *Physical Review X*, 8:011006, 2018.
- [GRK⁺20] A. Goeßmann, I. Roth, G. Kutyniok, M. Götte, R. Sweke, and J. Eisert. Tensor network approaches for data-driven identification of non-linear dynamical laws. *NeurIPS2020 - Tensorworkshop*, 2020. arXiv:2002.12388.
- [GSP⁺19] I. Glasser, R. Sweke, N. Pancotti, J. Eisert, and J. I. Cirac. Expressive power of tensor-network factorizations for probabilistic modeling, with applications from hidden markov models to quantum machine learning. *Advances in Neural Information Processing Systems 32, Proceedings of the NeurIPS 2019 Conference*, 2019. arXiv:1907.03741.
- [GST21] M. Götte, R. Schneider, and P. Trunschke. A block-sparse tensor train format for sample-efficient high-dimensional polynomial regression. *Frontiers in Applied Mathematics and Statistics*, 7:57, 2021.
- [HLO⁺16] J. Haegeman, C. Lubich, I. Oseledets, B. Vandereycken, and F. Verstraete. Unifying time evolution and optimization with matrix product states. *Physical Review B*, 94:165116, 2016.
- [HMOV14] J. Haegeman, M. Mariën, T. J. Osborne, and F. Verstraete. Geometry of matrix product states: Metric, parallel transport and curvature. *Journal of Mathematical Physics*, 55:021902, 2014.
- [IMW⁺20] R. Iten, T. Metger, H. Wilming, L. del Rio, and R. Renner. Discovering physical concepts with neural networks. *Physical Review Letters*, 124:010508, 2020.
- [KBK22] K. Kaheman, S. L. Brunton, and J. N. Kutz. Automatic differentiation to simultaneously identify nonlinear dynamics and extract noise probability distributions from data. *Machine Learning: Science and Technology*, 3:015031, 2022.
- [KG19] S. Klus and P. Gelß. Tensor-based algorithms for image classification. 2019. arXiv: 1910.02150.
- [LYCS17] Y. Levine, D. Yakira, N. Cohen, and A. Shashua. Deep learning and quantum entanglement: Fundamental connections with implications to network design. arXiv:1704.01552 [quant-ph], 2017.
- [MBPK16] N. M. Mangan, S. L. Brunton, J. L. Proctor, and J. N. Kutz. Inferring biological networks by sparse identification of nonlinear dynamics. 2016. arXiv: 1605.08368.
- [Oru14] R. Orus. A practical introduction to tensor networks: Matrix product states and projected entangled pair states. *Annals of Physics*, 349:117–158, 2014.
- [RCR⁺20] M. Riemer, I. Cases, C. Rosenbaum, M. Liu, and G. Tesauero. On the role of weight sharing during deep option learning. 2020. arXiv:1912.13408 [cs, stat].
- [SBK21] D. E. Shea, S. L. Brunton, and J. N. Kutz. Sindy-bvp: Sparse identification of nonlinear dynamics for boundary value problems. *Physical Review Research*, 3:023255, 2021.
- [SL09] M. Schmidt and H. Lipson. Distilling free-form natural laws from experimental data. *Science*, 324:81–85, 2009.
- [SPV10] S. Singh, R. N. C. Pfeifer, and G. Vidal. Tensor network decompositions in the presence of a global symmetry. *Physical Review A*, 82:050301, 2010.
- [SS16] E. Stoudenmire and D. J. Schwab. Supervised learning with tensor networks. *Advances in Neural Information Processing Systems*, 29, 2016.

- [SWVC08] N. Schuch, M. M. Wolf, F. Verstraete, and J. I. Cirac. Entropy scaling and simulability by matrix product states. *Physical Review Letters*, 100:030504, 2008.
- [VC04] F. Verstraete and J. I. Cirac. Renormalization algorithms for quantum-many body systems in two and higher dimensions. 2004. arXiv:cond-mat/0407066.
- [VC06] F. Verstraete and J. I. Cirac. Matrix product states represent ground states faithfully. *Physical Review B*, 73:094423, 2006.
- [VMC08] F. Verstraete, V. Murg, and J. I. Cirac. Matrix product states, projected entangled pair states, and variational renormalization group methods for quantum spin systems. *Advances in Physics*, 57:143–224, 2008.

A Conditions on low-rankness

In this appendix, we will discuss conditions on low-rankness and connect the ideas occurring in the mathematics and physics literature. We will hence provide evidence and a mathematical underpinning why the local function dictionaries picked often capture locally interacting physical systems exhibiting natural correlation patterns.

Let $u(x_1, \dots, x_d)$ be a multivariate L^2 function. Its coefficient tensor in a suitable product basis can always be written exactly in a tensor train format by iteratively performing a *singular value decomposition* (SVD) on its matricifications. *Proposition 5.1* in Ref. [BSU16] furthermore states, that it can be approximated by a lower rank tensor train $\tilde{u}(x_1, \dots, x_d)$ with error bounded by

$$\|u - \tilde{u}\|_2 \leq C\sqrt{d}\|u\|_{w\ell_*^p} \left(\max_{\eta \in \mathbb{E}} \text{rank}_\eta(\tilde{u}) \right)^s \quad (30)$$

for $0 < p < 2$, where $C > 0$ is a constant,

$$s := \frac{1}{p} - \frac{1}{2}, \quad (31)$$

\mathbb{E} is the set of edges of the tensor train,

$$\|u\|_{w\ell_*^p} := \max_{\eta \in \mathbb{E}} \|\sigma^\eta(u)\|_{w\ell^p} \quad (32)$$

with $\|\cdot\|_{w\ell^p}$ the weak- ℓ^p -norm and $\sigma^\eta(u)$ the tuple of singular values of the matricification of u 's coefficient tensor corresponding to the edge η . In particular, we are interested in approximations \tilde{u} , such that as d increases, the number of coefficients in the tensor train does not scale exponentially. This is closely related to *entanglement entropy scaling*, ubiquitous in the physics literature [SWVC08, ECP10].

Abstracting away from the L^2 space to a general p^d dimensional Hilbert space, we can think of u as a pure quantum state vector $|\psi\rangle$ of d qudits, which each have an associated p dimensional Hilbert space. This allows us to relate the ℓ^p norm corresponding to the edge η to the Rényi entropy

$$S_\alpha(\rho_\eta) := \frac{\text{tr}(\rho_\eta^\alpha)}{1 - \alpha} \quad (33)$$

of the reduced state $\rho_\eta := \text{tr}_\eta |\psi\rangle\langle\psi|$, where the subscript on the partial trace indicates that it is performed over the second part of the system, when it is split according to the edge η . Since, following the usual Schmidt decomposition procedure, the eigenvalues of ρ_η are just the squares of the singular values $\sigma^\eta(u)$, we get

$$S_\alpha(\rho_\eta) = \frac{2\alpha}{1 - \alpha} \log \|\sigma^\eta(u)\|_{2\alpha}. \quad (34)$$

We set $D := \max_{\eta \in \mathbb{E}} \text{rank}_\eta(\tilde{u})$. This quantity is often referred to as the *bond dimension* in the physics literature. We set also $L(\eta) \in \mathbb{N}$ to be the length of the first part of the system corresponding to the edge η .

Now consider a whole family $(|\psi_d\rangle)$ of such state vectors on systems of increasing d . For the tensor train formulation to be useful we require that for any $\delta > 0$ we can find a family $(|\tilde{\psi}_d\rangle)$ such that $\| |\psi_d\rangle - |\tilde{\psi}_d\rangle \|_2 \leq \delta$ for all d , such that $D(d) = \text{poly}_\delta(d)$. Rearranging Eq. (30), using Eq. (34) and the fact that

$$\|\cdot\|_{w\ell^p} \leq \|\cdot\|_{\ell^p}, \quad (35)$$

we get this is always possible if for some $0 < \alpha < 1$

$$\max_L S_\alpha(\rho_\eta^\alpha) \leq A \log \frac{A'}{\sqrt{d}} + B \log [\text{poly}_\delta(d)], \quad (36)$$

where A, A' and B are positive constants given by C, δ and α . This is precisely the first row of *Table 1* in Ref. [SWVC08].